JOURNAL OF CATALYSIS 81, 489–498 (1983)

Mechanism of Nitrogen Insertion in Ammoxidation Catalysis[1]

The selective ammoxidation of propylene in Eq. (1), that is, oxidation in the presence of NH_3, is the process by which more than 8 billion pounds of acrylonitrile per year are produced worldwide. The mechanistically similar oxidation reaction (Eq. (2)) produces acrolein, and generally occurs over the same catalysts, including bismuth molybdates ($Bi_2O_3 \cdot nMoO_3$, $n = 1, 2, 3$), uranium antimonate (USb_3O_{10}), iron antimonate (Fe_2O_3/Sb_2O_4), and bismuth molybdate-based multicomponent systems, which provide many of today's highly selective commercial catalysts. This work will center on the bismuth molybdate systems.

$$CH_3CH{=}CH_2 + NH_3 + 3/2\ O_2 \xrightarrow{400\text{-}460^\circ C} CH_2{=}CHCN + 3H_2O \quad (1)$$

$$CH_3CH{=}CH_2 + O_2 \xrightarrow{300\text{-}450^\circ C} CH_2{=}CHCHO + H_2O \quad (2)$$

The mechanism of the reactions has recently been reviewed (*1–5*). It has been well established that the reaction occurs via rate-determining hydrogen abstraction to produce an allylic intermediate (*6–8*) (Scheme 1). Substituent effect experiments (*9*) and reaction of allyl radicals over selective oxidation catalysts indicate that this allylic intermediate resembles a radical-like species. The subsequent reactions which formally insert O to form acrolein have been studied by the use of allyl alcohol as a probe molecule (*11*). The steps involved in N insertion, if NH_3 is present, to form acrylonitrile are less well understood and will be the main topic of this work.

[1] Presented at the Symposium on General Papers on Catalysis and Related Topics of Colloid and Surface Division, 183rd ACS National Meeting, Las Vegas, Nev., March 29, 1982.

While the catalytically active site for selective oxidation has not been firmly established, several key findings are informative. Correlation of ESCA data with catalytic activity by Grasselli *et al.* (*2*) and Matsuura (*12*) suggest that the active surface sites for selective oxidation in bismuth molybdate catalysts consist of bismuth–molybdenum pairs, i.e., surface Bi:Mo ratio is 1. It is also believed that the oxygens associated with Bi are responsible for allylic H abstraction, while oxygen polyhedra around Mo are inserted into the allylic intermediate (*10, 12, 13*).

In addition, the importance of Mo=O double bonds at the selective catalytic site has been noted by several workers. The presence of the Mo=O functionality as a key component for selectivity in several heterogeneous oxidation catalysts has been

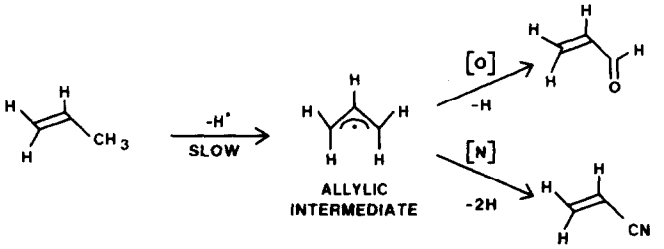

SCHEME 1. Selective propylene ammoxidation/oxidation mechanism.

0021-9517/83 $3.00

observed by Trifiro (*14*). Iwasawa (*15*) has found that the coordinately unsaturated tetrahedral dioxo structure is an essential component in structurally fixed Mo catalysts for selective oxidation of propylene. These experimental results are supported by the theoretical work of Goddard (*16*), which favors a dioxo molybdate over a monoxo species as an active site for olefin oxidation.

These findings can be accommodated by an active site structure **1** (Scheme 2) in which an H-abstracting oxygen associated with bismuth is bonded through a bridging O to the O-inserting Mo-dioxo group. This H-abstracting site is represented in Scheme 2, for simplicity, as a Bi=O group, but probably more closely resembles a bridging Bi–O moiety (Scheme 4). This site reacts with propylene to form the π-O-allylic intermediate **2** in the rate determining step. The insertion of oxygen via reversible C–O bond formation generates the σ form **3**, and activates the allylic hydrogens in the second H-abstraction step to form acrolein. Generation of a σ-O-allylic intermediate from allyl alcohol (*11*), or by reaction of ethanol with a fixed Mo-dioxo species (*17*) results in conversion to selective dehydrogenated products (i.e., acrolein and acetaldehyde, respectively). In light of spectroscopic observations of π- and σ-O bonded allyl structures during the selective oxidation of propylene over Mo-containing catalysts (*18*), the **1** → **2** → **3** scheme for the selective oxidation of propylene to acrolein is strongly suggested (Scheme 2).

In ammoxidation, initial activation of ammonia via condensation with terminal Mo=O groups then leads to the analogous α-H abstraction via **4**, to form π(**5**) and σ(**6**) N-bonded allylic intermediates. This scheme (Scheme 2) suggests the use of ammonia with either propylene, allyl alcohol, or allyl amine as molecular probes for this mechanism. The effect of ammonia on propylene ammoxidation kinetics and product distribution can give information concerning the N-insertion steps, using the oxidation sequence as a comparison. In addition, allyl alcohol and allyl amine ammoxidation can serve as independent methods of generating the σ-*N*-allylic species for subsequent study.

EXPERIMENTAL

All experiments were performed by the pulse method using a microreactor system interfaced with a gas chromatograph previously described (*10*), except for measurement of acrylonitrile : acrolein ratio dependence on $NH_3 : C_3H_6$, which was performed in a continuous flow integral reactor operating at steady state and less than 4% conversion (Fig. 3). For these latter experiments, the catalyst ($Ma^{2+}Mb^{3+}Bi_xMo_yO_z$) was

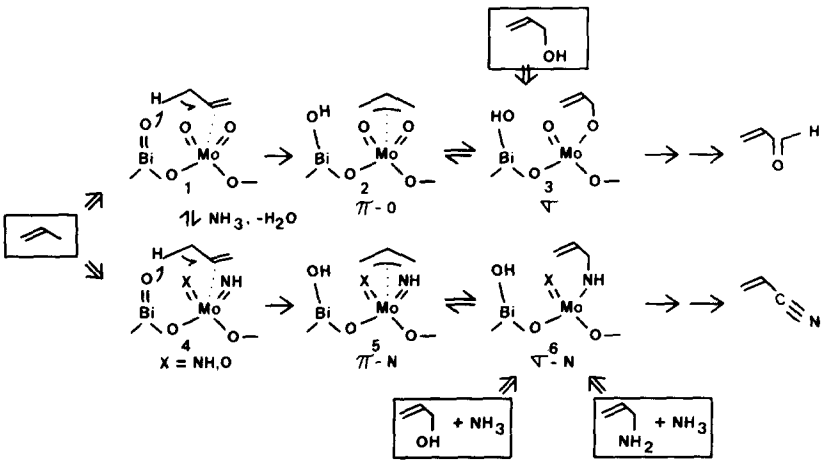

SCHEME 2. Molecular probes for O- and N-insertion.

equilibrated at 430°C, using a 1.0 C_3H_6: 1.2 NH_3: 11.0 air feed until steady state performance was achieved (at least 24 h). The catalyst was then cooled to 320°C, and the NH_3: C_3H_6 ratio adjusted to the desired level and left on stream for at least 30 min prior to the acrylonitrile : acrolein measurement (60- to 90-min recovery run), during which time constant performance was achieved. Results are recorded in Fig. 3. Analysis of the extent and position of the deuteration was derived from a combination of proton nuclear magnetic resonance (NMR) and mass spectral analysis using the instruments previously described (*11*). Catalysts used were unsupported fixed-bed (20–35 mesh) materials prepared by known methods (*11*). Deuterated propylenes were obtained commercially (Merck, Canada); 1,1-d_2- and 3,3-d_2-allyl alcohol, (*11*), and 1,1-d_2-allyl amine (*21*) were prepared by known routes. Unlabeled propylene (Matheson), allyl alcohol, and allyl amine were also obtained commercially. Experimental parameters for ammoxidation of propylene, allyl alcohols, or allyl amine are shown in Figs. 5–7.

RESULTS AND DISCUSSION

A. *Propylene as Probe*

There are several key similarities between oxidation and ammoxidation (Fig. 1). Both reactions produce the same relative rates and isotopic distribution of allylic oxygen- and nitrogen-insertion products from either allyl or vinyl D-labeled propylenes, indicating a k_H/k_D of 1.82 (*7*), which is nearly the theoretical maximum at this reaction temperature. Also, both reactions have the same overall activation energy, suggesting a similar rate determining step (α-H abstraction) (*19, 20*).

Effect of ammonia on activity and selectivity. The presence of ammonia, however, produces a number of effects (Fig. 2) (*2*). Typical temperatures required for ammoxidation are higher than those for oxidation. At 320°C, over a multicomponent bismuth molybdate catalyst, oxidation activity is high, but declines rapidly as ammonia is added. However, at 430°C, conversion remains high with increasing ammonia : propylene ratio. Selectivity (to acrylonitrile and acrolein) decreases slightly at 320°C and increases slightly at 430°C as ammonia is added (*2*).

Effect of ammonia on O/N–insertion product ratio. In an ammonia activation/nitrogen-insertion scheme, which follows the model shown in Scheme 2, the steps involved at the surface Mo site **7** (below), which is a generalized form of site **1** from Scheme 2, are

$$x\mathrm{NH_3} + \underset{\mathbf{7}}{\mathrm{Mo^{6+}(O)_2}} \xrightarrow{k_{AA}} \underset{\mathbf{8}}{\mathrm{Mo^{6+}(O)_{2-x}(NH)_x}} + x\mathrm{H_2O} \quad (3)$$

$$\mathrm{C_3H_6} + \underset{\mathbf{8}}{\mathrm{Mo^{6+}(O)_{2-x}(NH)_x}} + (\mathrm{O})_{\mathrm{lattice}} \xrightarrow[(\mathrm{Bi\text{–}O})]{-\mathrm{H},k_{NI}} \mathrm{C_3H_3N} + \mathrm{Mo^{3+}} + (x-1)\mathrm{NH_3} + (3-x)\mathrm{H_2O} + [\mathrm{O_v}] \quad (4)$$

$$\mathrm{Mo^{3+}} + 1.5[\mathrm{O}]_{\mathrm{lattice}} \xrightarrow{k_{diff}} \mathrm{Mo^{6+}(O)_2} + 1.5[\mathrm{O_v}] \quad (5a)$$

$$2.5[\mathrm{O_v}] + \tfrac{5}{4}\,\mathrm{O_2(g)} \xrightarrow{k_{ox}} 2.5[\mathrm{O}]_{\mathrm{lattice}} \quad (5b)$$

where Eq. (3) represents ammonia activation, (4) is nitrogen insertion, (5a,b) catalyst reoxidation, and $[O_v]$ an oxygen vacancy in the oxide lattice. The corresponding oxidation reaction involves O insertion (6), followed by reoxidation (5a,b).

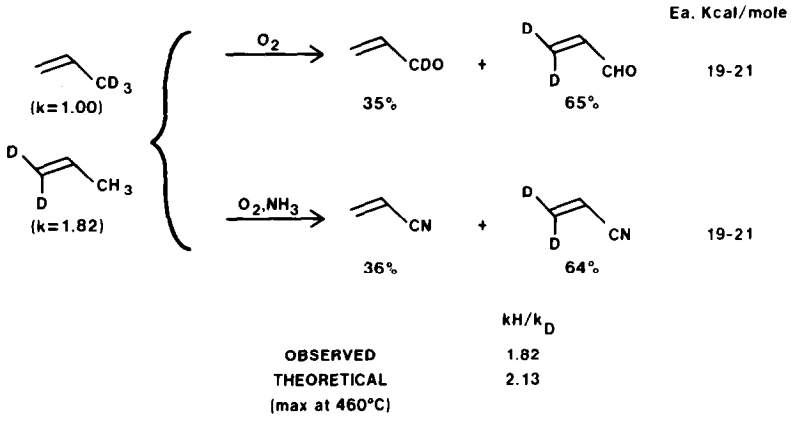

FIG. 1. Comparison of oxidation and ammoxidation, $Bi_2Mo_3O_{12}$ catalyst, 460°C; see Refs. (*7, 11*).

$$\underset{7}{Mo^{6+}(O)_2} + C_3H_6 \xrightarrow[(Bi\text{–}O)]{-H^\circ, k_{OI}} Mo^{3+} + C_3H_4O + H_2O. \quad (6)$$

Of course, the above equations (3)–(6) represent only overall kinetic expressions and are not mechanistically rigorous, since each equation may in fact be composed of a number of steps. Also, since k_{diff} and k_{ox} in the reoxidation sequence (Eqs. (5a), (5b)) are greater than k_{NI} or k_{OI}, the existence of discrete Mo^{3+} reduced species as represented in Eqs. (4) and (6) is unlikely.

Based on the above Eqs. (4) and (6), the ratio of the rates of formation of acrylonitrile and acrolein may be expressed as

$$\frac{r(C_3H_3N) = k_{NI}(C_3H_6)(\mathbf{8})[O]}{r(C_3H_4O) = k_{OI}(C_3H_6)(\mathbf{7})}\ \text{lattice}. \quad (7)$$

Applying the steady state approximate for **8**, where

$$k_{NI}(C_3H_6)(\mathbf{8})[O]_{lattice} = k_{AA}(NH_3)^x(\mathbf{7}) \quad (8)$$

gives

$$\frac{r(C_3H_3N) = k_{AA}(NH_3)^x(\mathbf{7}) = (k_{AA})(NH_3)^x}{r(C_3H_4O) = k_{OI}(C_3H_6)(\mathbf{7}) = (k_{OI})(C_3H_6)}. \quad (9)$$

Thus, a plot of the product acryloni-

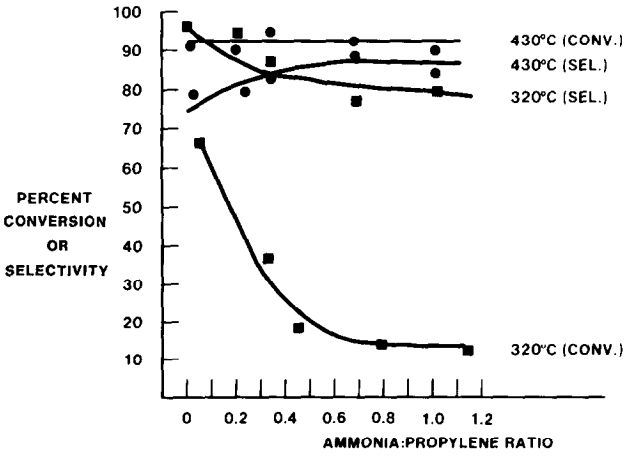

FIG. 2. Catalytic pulse oxidation of propylene (C_3H_6) as a function of ammonia: propylene ratio. 3 μmol C_3H_6/pulse, 0.92 g (1 cc) catalyst $(M_a^{2+}M_b^{3+}Bi_xMo_yO_z)^{11}$, 1 s contact time; see Ref. (*2*). Feed = $C_3H_6 : NH_3 : He : air = 1 : 1.2 - x : x : 11.0$. SEL = acrolein + acrylonitrile selectivity.

trile : acrolein ratio vs the molar feed ratio $(NH_3)^x/C_3H_6$ should give a straight line with slope equal $(1/n)^{x-1}(k_{AA}/k_{OI})$, where x molecules of ammonia react at each nitrogen insertion site per catalytic cycle and n = total number of moles in the gas phase feed, based on $C_3H_6 = 1.0$.

The acrylonitrile : acrolein product ratio is a linear function of $(NH_3)^2/C_3H_6$ ratio (Fig. 3) (*21*). A plot of the acrylonitrile : acrolein product ratio vs NH_3^2/C_3H_6 exhibits two regions of linear behavior corresponding to $NH_3/C_3H_6 < 0.24$ with a slope of 100, and $NH_3/C_3H_6 > 0.24$ with a slope of 24.2. This indicates that there are two active N-insertion sites present on the multicomponent catalyst surface, having a relative (k_{AA}/k_{OI}) ratio of about 4 : 1, and both of which react with two molecules of ammonia in each catalytic cycle (i.e., $x = 2$ in Eq. 3).

Selectivity to acrylonitrile under ammoxidation conditions increases much more rapidly with temperature than that to acrolein under oxidation conditions in the 400–480°C temperature range. From the difference in the slopes in the Arrhenius plot (Fig. 4), the difference in E_a between selective and CO_2 formation is 9.3 kcal/mol for ammoxidation and 1.3 kcal/mol for oxida-

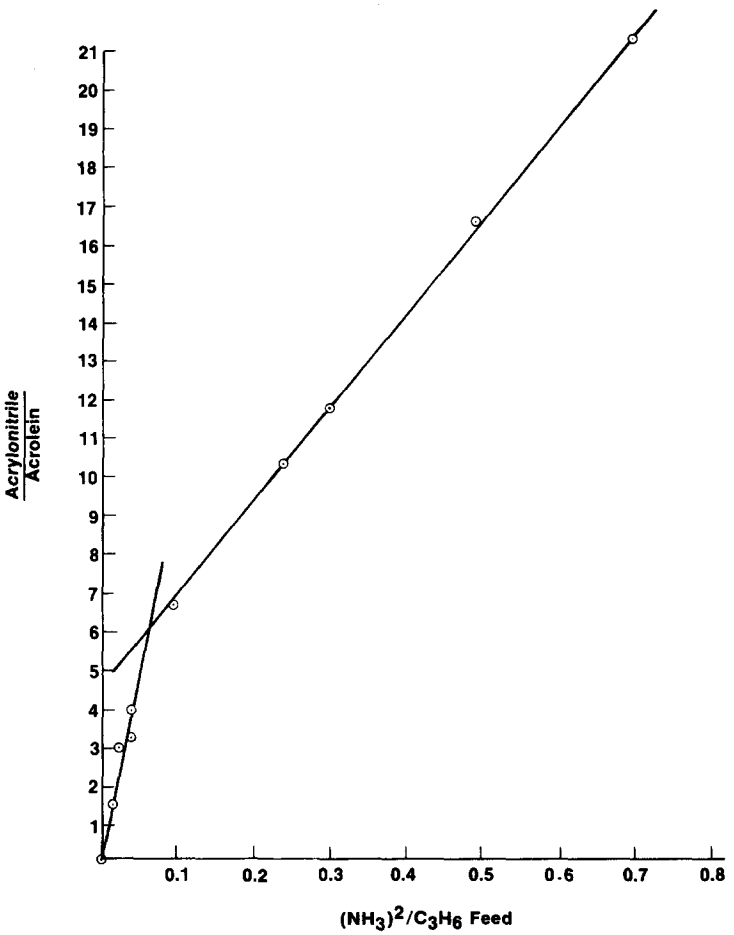

FIG. 3. Effect of NH_3/C_3H_6 ratio on acrylonitrile/acrolein ratio at 320°C over multicomponent molybdate catalyst. (a) 0.92 g (1.0 cc) catalyst $(M_a^{2+}M_b^{3+}Bi_xMo_yO_z)^{11}$ after equilibration with 1.0 C_3H_6 : 1.2 NH_3 : 11.0 air feed at 430°C, 24 h followed by 30-min prerun at 320°C; (b) feed = 1.0 C_3H_6 : $(1.2 - x)NH_3$: x He : 11.0 air; 1.0 s contact time.

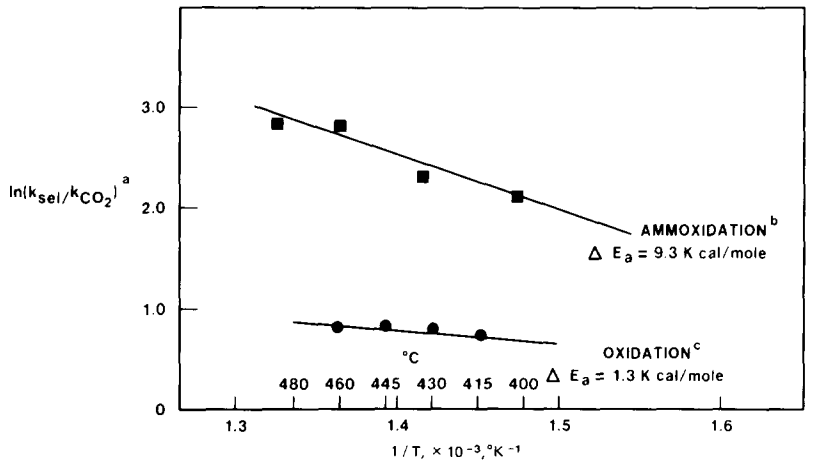

FIG. 4. Arrhenius dependence of selectivity on temperature for oxidation and ammoxidation over $Bi_2Mo_3O_{12}$. (a) 3.0–3.2 μ mol C_3H_6 per pulse, 2.0 g $Bi_2Mo_3O_{12}$, 15–30% C_3H_6 conversion; see Ref. (*2*). (b) 1.8 s contact time, feed ratio = 1.0 C_3H_6 : 2.6 O_2 : 8.7 He; (c) 1.4(480°C)–4.0(400°C) s contact time, feed ratio = 1.0 C_3H_6 : 2.5 O_2 : 5.0 NH_3 : 3.5 He.

tion. Assuming a similar CO_2-forming mechanism for both reactions, an activation energy difference of 8 kcal/mol results for the overall N vs O insertion process. This indicates that the *N*-allyl intermediate has a higher activation energy for conversion to acrylonitrile than for *O*-allyl conversion to acrolein.

B. Allyl Alcohol as Probe

Oxidation vs ammoxidation. The oxidation and ammoxidation of allyl alcohol has been studied in detail (*11*). The main oxidation products of these reactions are acrolein and acrylonitrile, respectively (Fig. 5). The one electron reductive dimerization product, 1,5-hexadiene, is also a major product under oxidation conditions (no ammonia). The formation of acrolein decreases and that of acrylonitrile increases with ammonia addition, as expected, but several mole equivalents of ammonia are required per al-

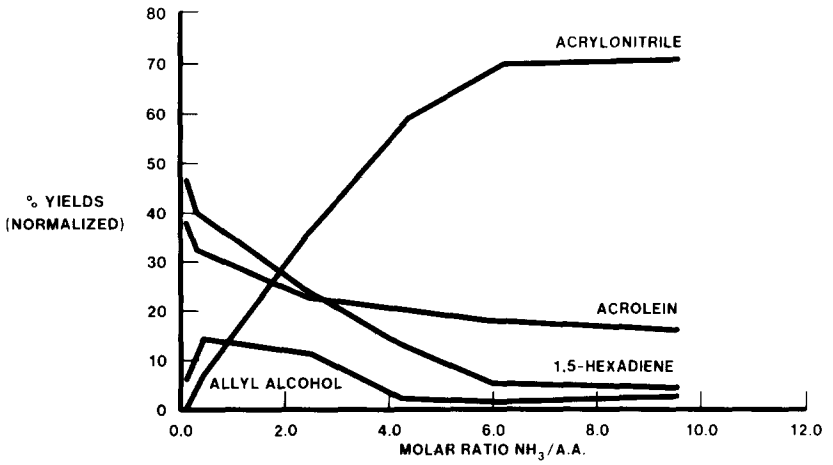

FIG. 5. Yield vs ammonia: allyl alcohol ratio (NH_3 : AA) for reaction with MoO_3 at 380°C; 3.5 μ mol (NH_3 + allyl alcohol) injected per pulse, 0.98 g (0.5 cc, 0.7 m^2) MoO_3, fresh catalyst used for each run; see Ref. (*11*).

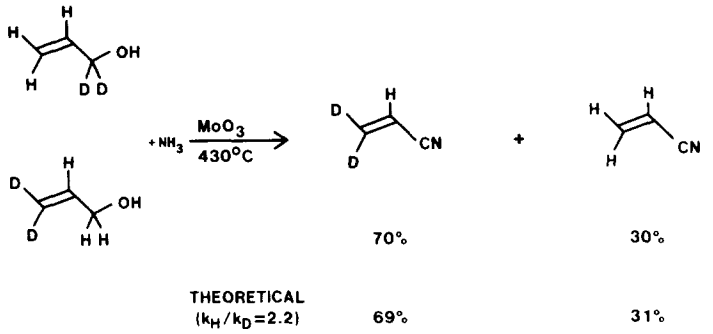

FIG. 6. Ammoxidation of 1,1-d_2 and 3,3-d_2 allyl alcohol. (a) NH_3 : allyl alcohol = 4.0 (30–45 μmol total) 2.0 s contact time, 5.2 g (2.9 cc, 4 m^2) MoO_3; see Ref. (*11*).

lyl alcohol in the gas phase to give the maximum yield of acrylonitrile.

Ammoxidation of 1,1-d_2 and 3,3-d_2 Allyl alcohol. The ammoxidation of either 1,1-d_2- or 3,3-d_2-allyl alcohol over molybdate catalysts (Fig. 6) gives the same product distribution (i.e., 70% d_2, 30% d_0) in which preferential abstraction of deuterium occurs, consistent with the theoretical maximum for k_H/k_D at 430°C of 2.2. This indicates that preferential H abstraction occurs from either end of the allylic intermediate produced from either allyl alcohol or propylene ammoxidation.

C. *Allylamine as Probe*

The behavior of allylamine as a probe molecule is very different from that of propylene or allyl alcohol. Besides acrylonitrile, propionitrile is formed in allylamine oxidation or ammoxidation as a major product (*19*), with smaller amounts of acetonitrile, propylene, and diallylamine (Fig. 7). The main effect of ammonia in this case is to function as a base rather than a nitrogen-inserting species, increasing propionitrile selectivity at the expense of acrylonitrile (*19*).

Also in contrast to propylene or allyl alcohol, allylic H abstraction is no longer the rate-determining step for reaction of allyl amine under either oxidation or ammoxidation conditions, since a similar conversion to products of either d_0 or 1,1-d_2 is observed.

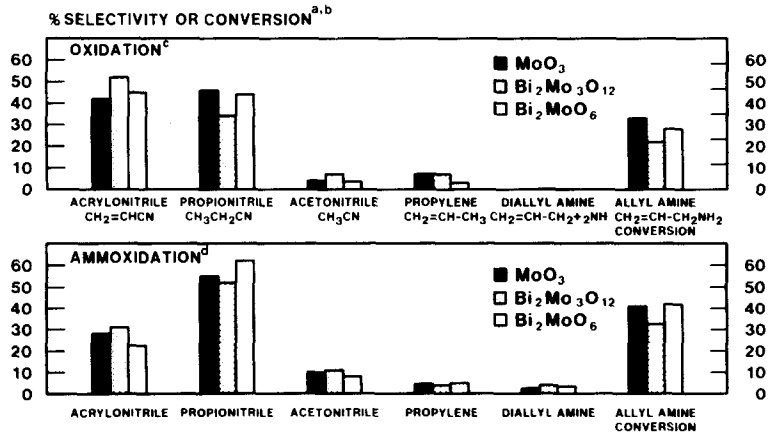

FIG. 7. Effect of Bi/Mo ratio in oxidation and ammoxidation of allylamine at 400°C (benzene diluent). (a) 3.0 cc catalyst, 5.8 s contact time, 21 μ mol allylamine injected; see Ref. (*21*). (b) Σ products observed; (c) no NH_3 in feed; (d) NH_3 : allyl alcohol (molar) = 4.5.

D. Mechanism

Allyl alcohol vs allyl amine. A mechanism consistent with the results for allyl alcohol ammoxidation (Scheme 3) involves initial condensation of the Mo-dioxo species **9** with two equivalents of ammonia to produce the diimido species **10**. Addition of allylamine to one of the diimido groups produces **11**, analogous to the addition of allyl alcohol to a dioxo species in oxidation of allyl alcohol (*11*). The 70 d_2 : 30 d_0 product distribution in which preferential allylic H abstraction occurs requires the formation of a symmetrical π-allylic intermediate, in which equal probability of C–N bond formation on either side of the allylic species occurs. This can be accommodated by the O to N migration, followed by tautomerization to form σ-allyl species **13a**, where the least hindered imido group (=NH) is formed, and subsequent rapid equilibration with isomeric form **13b**, the 3,3-d_2- and d_0-acrylonitrile precursors, respectively (via a formal 1,4-H shift). The rearrangements **11** → **12** and **13a** → **13b** could occur either by formation of a π-allyl (e.g., **14**) or via concerted [3,3] sigmatropic shift.

The 70 d_2 : 30 d_0 product distribution requires that reactions **11** → **12** and **12** → **13a** be essentially irreversible and faster than α-H abstraction. Since the bond energy difference (C–O) − (C–N) = 13 kcal/mol and that for (O–H) − (N–H) = 17 kcal/mol, the limits for the π-bond component of the difference (Mo-oxo)-(Mo-imido) are 13–17 kcal/mole if both **11** → **12** and **12** → **13a** are thermodynamically favored. Such Mo^{6+} monoxo or monoimido species have triple bond character, and are responsible for the spectator stabilization suggested by Goddard (*16*) who estimates the effect to be about 13 kcal/mol greater for the oxo than for the imido group, consistent with the above limits.

Allylamine, however, successfully competes with ammonia for molybdate sites to produce the *N*-allyl oxo species **15**, which undergoes rapid tautomerization to the imido hydroxy species **16** (analogous to the **12** → **13a** reaction) and subsequent dehydration to form imidooxo complex **17**, the precursor to acrylonitrile, where the C–N bond originally in allylamine remains intact.

Mechanism of Ammoxidation and Oxidation of Propylene over Bismuth Molybdate Catalysts. The active surface species **18** common to both reactions (Scheme 4) is composed of a bridging (Bi–O) which is the

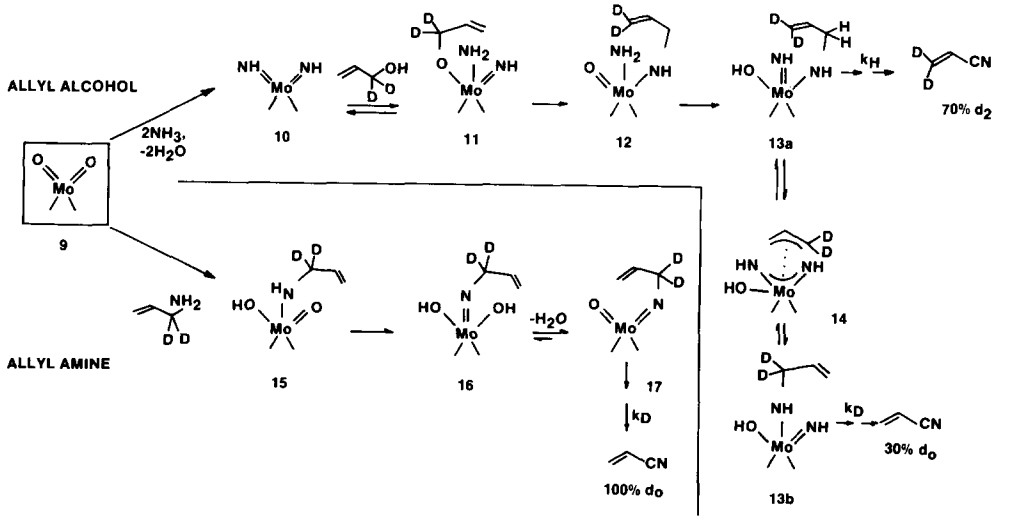

SCHEME 3. Mechanism of allyl alcohol and allyl amine ammoxidation over molybdate catalysts.

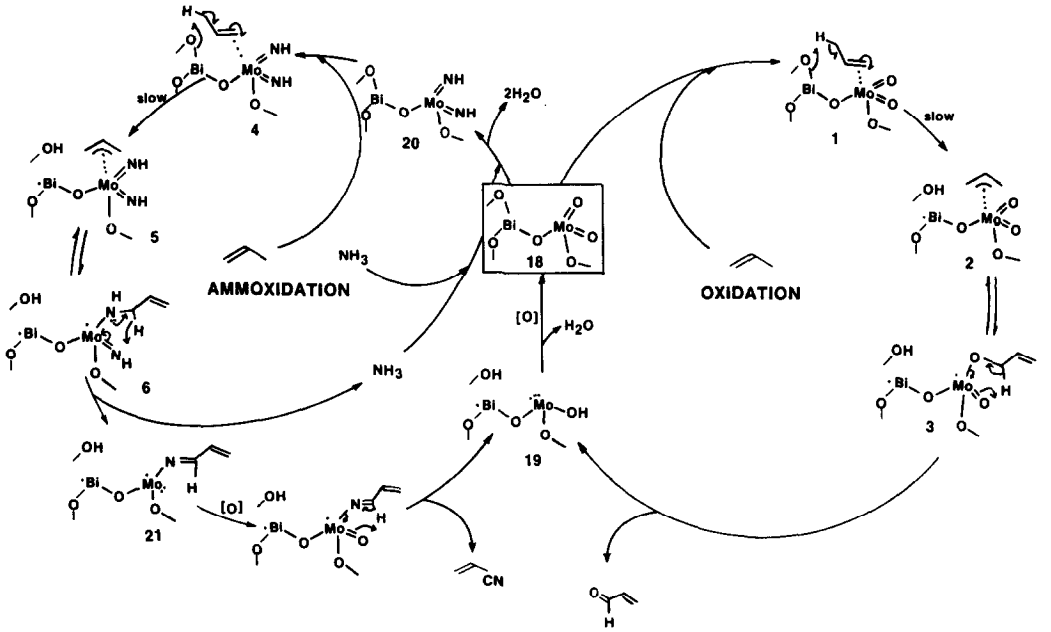

SCHEME 4. Mechanism of selective ammoxidation and oxidation of propylene over bismuth molybdates.

allylic hydrogen abstraction component, and a molybdenum dioxo functionality which serves as the site for propylene chemisorption, and for oxygen insertion in oxidation and ammonia activation and nitrogen insertion in ammoxidation. In oxidation, initial chemisorption and α-H abstraction produces the π-allyl species **2** followed by reversible σ-species (**3**) formation and second H abstraction, formally a 1,4-H shift, to produce acrolein and reduced surface site **19**. This site undergoes reoxidation to reform the active site **18** by migration of lattice O^{2-} from the bulk and subsequent chemisorption of molecular O_2 at another reduced site.

In ammoxidation, ammonia activation by formation of the diimido species **20** first occurs followed by analogous formation of π(**5**) and σ(**6**) forms. However, the intermediate imido species **21**, formed after the second H abstraction, a process which liberates one ammonia molecule per site, remains chemisorbed during the reoxidation step and undergoes a third H abstraction to form acrylonitrile and reduced site **19**, which undergoes reoxidation as before. Each cycle requires two ammonia molecules for formation of the active diimido nitrogen insertion species, one from the feed, and one liberated in the previous cycle, accounting for the linear (acrylonitrile : acrolein) dependence on $(NH_3)^2/C_3H_6$. Also, in the ammoxidation cycle, the higher increase in selectivity with increasing temperature is due to the higher activation energy for the second H abstraction in the σ-*N*-allyl complex (**6**) compared to the *O*-allyl (3). This is likely due to the lower reducibility of **6** compared to **3** and the lower H-abstracting ability of the imido group in **6**. This second H abstraction is the rate-determining step in the conversion of the σ-allyls to selective products. The ammonia inhibition of propylene ammoxidation at temperatures below 400°C can be explained by the initial formation of an inactive $Mo^{6+}(O)(OH)(NH_2)$ species, which requires temperatures greater than 400°C for conversion to **20**.

E. Conclusions

From this work, several general conclu-

sions can be drawn about the mechanism of olefin ammoxidation and the chemistry of the surface intermediates related to this process. First, selective olefin oxidation and ammoxidation involve initial rate-determining α-H abstraction to form analogous π-allyl complexes, and, subsequently, the σ-allyl species. Second, the active N-insertion center is composed of a coordinately unsaturated Mo diimido complex. Third, the activation energy for the conversion of the corresponding π-allyl species to selective ammoxidation products is higher than for conversion to selective oxidation products, resulting in greater increase in selectivity with increasing temperature for ammoxidation. Last, rapid O to N migration of C, and N to O migration of H, results in formation of Mo-oxo-amino (**12**) and hydroxy-imido (**16**) intermediates in allyl alcohol and allylamine ammoxidation, respectively. These transformations produce a symmetrical allylic intermediate for allyl alcohol, but result in C–N retention in allylamine ammoxidation.

REFERENCES

1. Grasselli, R. K., and Burrington, J. D., *in* "Advances in Catalysis," Vol. 30, p. 133. Academic Press, New York, 1981.
2. Grasselli, R. K., Burrington, J. D., and Brazdil, J. F., *J. Chem. Soc. Faraday Discuss.* **72,** 203 (1982).
3. Haber, J., and Bielanski, A., *Catal. Rev. Sci. Eng.* **19,** 1 (1979).
4. Keulks, G. W., and Krenzke, L. D., *in* "Advances in Catalysis," Vol. 27, p. 183. Academic Press, New York, 1978.
5. Gates, B. C., Katzer, J. R., and Schuit, G. C. A., "Chemistry of Catalytic Processes," pp. 325–389, McGraw–Hill, New York.
6. Sachtler, W. M. H., and de Boer, N. H., *in* "Proceedings, 3rd International Congress on Catalysis, Amsterdam, 1964," p. 252. Wiley, New York, 1965.
7. Adams, C. R., and Jennings, T., *J. Catal.* **2,** 63 (1963); Adams, C. R., and Jennings, T., *J. Catal.* **3,** 549 (1964); Adams, C. R., Voge, H. H., Morgan, C. Z., and Armstrong, W. E., *J. Catal.* **3,** 379 (1964).
8. Grasselli, R. K., and Suresh, D. D., *J. Catal.* **25,** 273 (1972).
9. Burrington, J. D., Kartisek, C. T., and Grasselli, R. K., *J. Org. Chem.* **46,** 1877 (1981); *J. Catal.* **69,** 495 (1981).
10. Burrington, J. D., and Grasselli, R. K., *J. Catal.* **59,** 79 (1979).
11. Burrington, J. D., Kartisek, C. T., and Grasselli, R. K., *J. Catal.* **63,** 235 (1980).
12. Matsuura, I., Schut, R., and Hirakawa, K., *J. Catal.* **63,** 152 (1980).
13. Greybowska, B., Haber, J., and Janas, J., *J. Catal.* **49,** 150 (1977); Sokolouskii, V. D., and Bulgakov, N. N., *React. Kinet. Catal. Lett.* **6,** 65 (1977).
14. Trifiro, F., and Italo, P., *J. Catal.* **12,** 412 (1968); Trifiro, F., *Chem. Ind. (Milan)* **56,** 835 (1974).
15. Iwasawa, Y., Nakamura, T., Takamatsu, K., and Ogasawara, S., *J. Chem. Soc. Faraday Trans. 1* **76,** 939 (1980).
16. Rappe, A. K., and Goddard, W. A., III, *J. Amer. Chem. Soc.* **104,** 448 (1982).
17. Iwasawa, Y., Nakano, Y., and Ogasawara, S., *J. Chem. Soc. Faraday Trans. 1* **74,** 2968 (1978).
18. Davydov, A. A., Mikhaltchenko, V. G., Sokolovskii, V. D., and Boreskov, G. K., *J. Catal.* **55,** 299 (1978).
19. Callahan, J. L., Grasselli, R. K., Milberger, E. C., and Strecker, H. A., *Ind. Eng. Chem. Prod. Res. Dev.* **9,** 134 (1970).
20. Schuit, G. C. A., *J. Less Common Met.* **36,** 329 (1974).
21. Burrington, J. D., Kartisek, C. T., and Grasselli, R. K., *J. Catal.* **75,** 225 (1982).

J. D. BURRINGTON
C. T. KARTISEK
R. K. GRASSELLI

Sohio Research Center
4440 Warrensville Center Road
Cleveland, Ohio 44128

Received September 20, 1982